

GAS BREAKDOWN MITIGATION IN SATELLITE SLIP-RINGS

F. Avino*, D. Bommottet†, B. Gaffinet*, A.A. Howling*, P. Martens*, and I. Furno*

*Swiss Plasma Center (SPC), Ecole Polytechnique Fédérale de Lausanne (EPFL), CH-1015 Lausanne, Switzerland.

†RUAG Space, CH-1260 Nyon, Switzerland.

ABSTRACT

The feasibility of increasing satellite bus voltages up to approximately 600 V is currently under investigation. This would allow implementing more powerful thrusters, to increase the power efficiency and to decrease the power system costs. One of the main disadvantages is given by the much higher risk of electrical breakdown. This work is devoted to the investigation of gas breakdown mitigation on the cylindrical design of the satellite slip ring assembly (SRA), in the framework of the High-Voltage Electrical Power System Architecture (HV-EPSA) project. The SRA features a complex geometry to ensure the electrical power transmission between the rotating solar panels and the main body of the satellite: gold-plated brushes slip on a stack of gold-plated rings, surrounded by a conducting housing at the ground reference voltage of the satellite. The experimental results of our newly-developed mitigation technique of gas breakdown in SRA mockups will be presented. Numerical studies in a simplified configuration, based on a fluid model developed with the COMSOL software to reproduce the breakdown condition, will be discussed. A new design of SRA will be introduced, together with the first experimental measurements on an advanced SRA mockup.

Key words: Satellite slip ring, electrical breakdown, Paschen's law, DC discharges, power transmission system.

1. INTRODUCTION

Electrical breakdown inhibition in satellite circuits is a technological challenge. Satellites experience a wide range of pressures during the de-pressurization phase, from atmospheric pressure before launch to high vacuum in orbit ($\sim 10^{-8}$ mbar). Also, many poorly-defined parameters characterise the environment surrounding a satellite during its operating life: pressure fluctuations could occur because of degassing, gas thrusters or micro-meteoroid impact, and a population of low energy ions could back-flow from an ion thruster plume. The satellite components that are mostly prone to electrical breakdown

are the solar panels [1], constituting the power source, and the slip ring assembly (SRA), which is part of the power transmission circuit of a satellite [2]. From present bus voltages in the range 28-100 V, evaluation of interest in using higher voltages in the range 300-600 V is under way, with the consequent higher risk of electrical breakdown. These voltages could be required to power new generations of ion and Hall effect thrusters [3]. Power efficiency could also be improved by reducing the operating currents in the power lines and the corresponding ohmic losses. Lower power system costs ($\sim 30\%$ cost reduction) and substantial mass savings ($\sim 50\%$ mass reduction) could be achieved.

This work focuses on gas breakdown on the standard cylindrical configuration of a SRA, which ensures the electrical power transmission between the rotating solar panels and the rest of the satellite via gold-plated brushes slipping on gold-plated rings. This geometry includes a stack of exposed biased conductors, surrounded by a conducting housing at the ground reference voltage of the satellite, as illustrated in Fig. 1 (a). Here, Direct-current (DC) breakdown is investigated by measuring the breakdown voltage as a function of pressure. Our aim is the optimization of the slip ring design to make it more robust with respect to gas breakdown.

In Sec. 2, measurements with a simplified SRA mockup are presented to introduce our new technique to inhibit gas breakdown [4]. The screening effect of grounded limiting discs for pressures lower than 1 mbar is first discussed with experimental measurements, and qualitatively confirmed with numerical fluid simulations. This design leads to an improvement in terms of pressure range of safe operation, but does not increase the minimum of the breakdown voltage.

A new design with passively-biased limiting discs is then presented, where the minimum of the breakdown curve is increased. Preliminary results with an advanced SRA mockup are given in Sec. 3 to test the screening effect with a component reproducing the complex geometry of a real SRA. The conclusions are discussed in Sec. 4, with an outlook on the following steps towards a realistic SRA design robust with respect to electrical breakdown up to ~ 700 V.

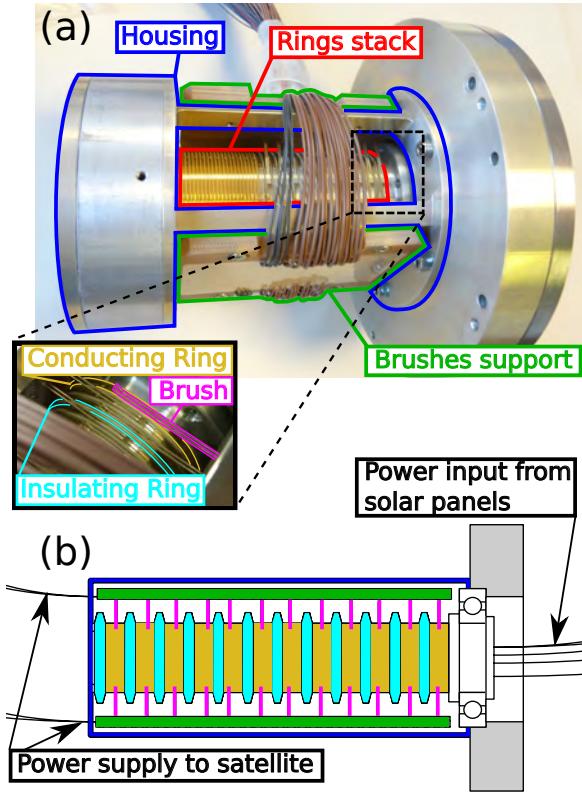


Figure 1. (a) Picture of a cylindrical slip ring for a satellite [5]. The conducting housing surrounding the ring stack is partially removed to expose the slip ring components. A detailed view of gold-plated brushes, gold-plated and insulating rings is shown. (b) Schematic of the slip ring with the colours of the components corresponding to those indicated in (a).

2. SIMPLE SRA MOCKUP

2.1. Experimental set-ups and procedure

A schematic of the experimental setup is shown in Fig. 2. Measurements are performed using air inside a grounded cylindrical stainless steel vacuum chamber, 32 cm diameter and 40 cm height. A minimum pressure of $\approx 5 \times 10^{-2}$ mbar can be attained by using a rotary pump. The pressure can be adjusted either by varying the pumping speed through a valve at the pump input, or by regulating the air flux with a valve on the vacuum chamber. Pressure measurements are performed in the range 1.3×10^{-2} - 13 mbar. A schematic and a photograph of the simplified SRA mockup we have developed are shown in Fig. 3(a) and 3(b). A stack of rings is composed of a central brass HV-ring, 1 mm thick, with an internal diameter of 34 mm and an external diameter of 38 mm. This is held between two adjacent insulating rings with the same dimensions, made of Vetrinite G-11, a material with a dielectric strength of 20 kV/mm. Two 0.2 mm thick brass discs of variable diameter enclose the assembly, which is held in the middle of the vacuum chamber by a Teflon

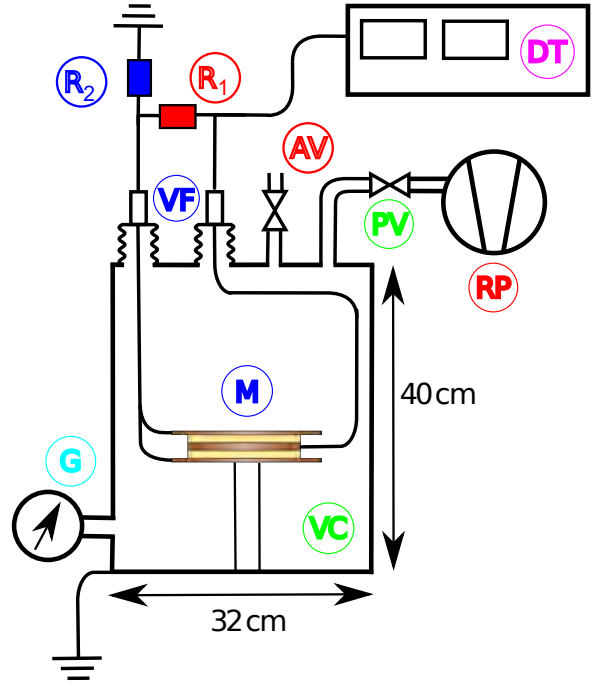


Figure 2. Schematic of the experimental setup. The mockup (M) is tested inside the steel vacuum chamber (VC). The pumping system includes a rotary pump (RP), a valve (PV) to regulate the pumping speed, and a valve (AV) to set the air flow from outside the chamber. The gauges used for the pressure measurements (G) are indicated. The dielectric tester (DT) and the HV vacuum feed-throughs (VF) used to bias the HV electrode are shown. The limiting discs are biased with respect to the HV electrode using the two resistances (R_1) and (R_2).

support. The central HV-ring is positively biased with respect to the ground potential of the chamber by a non-destructive insulation tester capable of reaching 30 kV. Three current (1, 10 and 100 μ A) and voltage (0-3, 0-10 and 0-30 kV direct current - DC) ranges provide a sufficient flexibility for the operating parameters. The limiting discs are connected to the HV electrode and to the ground via two resistances R_1 and R_2 to adjust their voltage, as shown in Fig. 2. The experimental procedure to measure the breakdown curves is the following: The initial pressure of $\approx 10^{-2}$ mbar is reached. The pressure is then increased by using the pressure valves. For each pressure, the voltage is manually increased with an average speed between 10 and 100 V/s to avoid over-voltage effects. Once breakdown occurs and the tester voltage can not be increased any more, the bias voltage is set back to zero and the pressure is increased. The breakdown voltage can be read directly on the tester meter.

2.2. Grounded Limiting Discs

Intuitively, electrical breakdown between electrodes can be avoided by increasing the inter-electrode gap. Although it is true for vacuum breakdown[2], gas break-

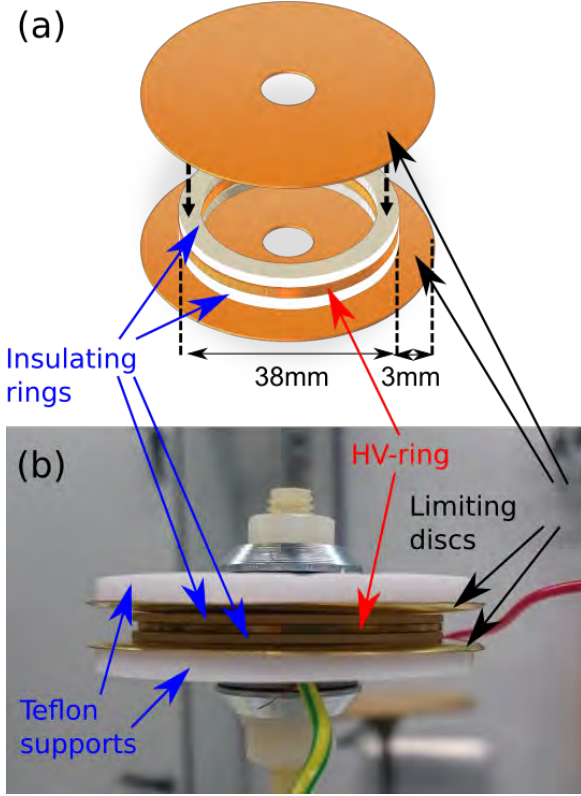


Figure 3. (a) Schematic of the setup. The central HV-ring (yellow) is isolated from the external limiting discs (yellow) by two insulating rings of Vetrinite (white). The top disc is raised to show the lower part of the stack. The insulating support filling the internal volume inside the rings is not shown. (b) Photograph of the assembly.

down occurs at lower voltages and along the electrical field path where the ionizing avalanche process is the most efficient, not necessarily along the shortest path. This is relevant in complex geometries like in a SRA, where the available breakdown paths range from the millimetre scale between adjacent rings, up to tens of centimetres between a HV ring and the surrounding conducting housing at the ground reference voltage of the satellite (Fig. 1). In our experimental investigations, the grounded vacuum chamber plays a role equivalent to that of the SRA housing. For low-enough pressures, a gas discharge between the HV ring and the surrounding vacuum chamber can be dominant.

In this section, we present the results obtained with our SRA mockup, keeping the limiting discs at the ground potential, which corresponds to $R_1 \rightarrow \infty$ and $R_2 \rightarrow 0$. The breakdown curves were measured for progressively increasing diameter of the discs. The chosen values are 38 mm, 40 mm, 44 mm, 48 mm and 58 mm. These diameters correspond to two conducting boundaries extending beyond the HV-ring radius by +0 mm, +1 mm, +3 mm, +5 mm, and +10 mm, respectively. The breakdown curve measurements in the range $p = 5 \times 10^{-3} - 10$ mbar are presented in Fig. 4. A maximum bias of 6 kV was applied to the HV-ring. The error-bars correspond to the resolu-

tion of the voltage meter, which is 100 V or 200 V for the values below or above 3 kV, respectively.

A first set of breakdown measurements was performed without the grounded discs. Comparing these results with those including the +0 mm discs reveals opposite trends at the two sides of the crossing point between the two curves (at $p \simeq 5 \times 10^{-1}$ mbar). The presence of the limiting grounded discs modifies the low-pressure branch, increasing the breakdown voltage. This effect can be related to the modified electric field spatial distribution that inhibits the discharge on long electric field paths towards the chamber walls, as shown in Sec. 2.3 with numerical simulations. On the other hand, the high-pressure range shows lower voltages due to the presence of short paths available with the inclusion of the discs. This last point is confirmed because all disc diameters give the same breakdown values at high pressures. We note that the curve without the grounded limiting discs (with only long path breakdown) will not occur in a real SRA, where the characteristic distance between the conducting rings in the stack is of the order of millimetres. The presence of progressively wider grounded surfaces

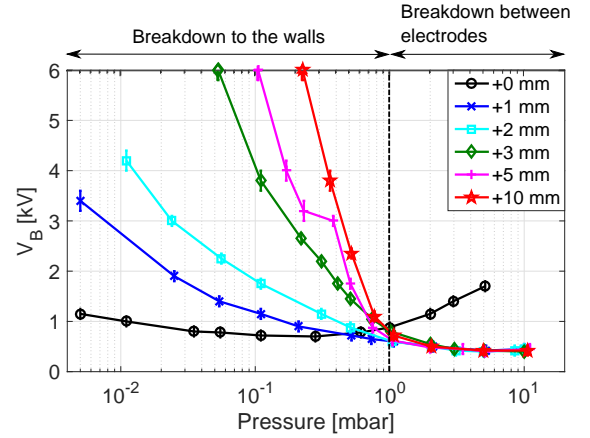


Figure 4. Breakdown voltage as a function of the gas pressure for different grounded discs. The black circles are for the HV-ring alone inside the vacuum chamber. The other measurements refers to the assembly with grounded limiting rings of increasing diameter.

enclosing the central HV-rings significantly increases the voltage for which the gas discharge occurs in the range $p = 5 \times 10^{-3} - 5 \times 10^{-1}$ mbar, as shown in Fig. 4. For an intermediate pressure of 10^{-1} mbar, the presence of grounded limiting discs 3 mm wider with respect to the central ring surface increases the breakdown voltage from ≈ 1 kV to ≈ 4 kV. We can see that for the +10 mm curve, gas breakdown is almost completely suppressed up to approximately 2×10^{-1} mbar, for applied voltages below 6 kV. This is a significant improvement compared to the standard slip-ring where all rings have the same diameter (+0 mm curve in Fig. 4) and therefore constitutes a new technical solution to inhibit gas breakdown from the HV ring to the surrounding housing.

In Sec. 2.3, numerical simulations are presented to shed light on the physical mechanism and relevant parameters responsible for the observed breakdown curves.

2.3. Numerical simulations

To further investigate the experimental results obtained in Sec. 2.2, numerical studies were performed with the finite element software COMSOL 4.2 [7]. A two-dimensional axisymmetric model is implemented, with a schematic shown in Fig. 5. The vertical axis of symme-

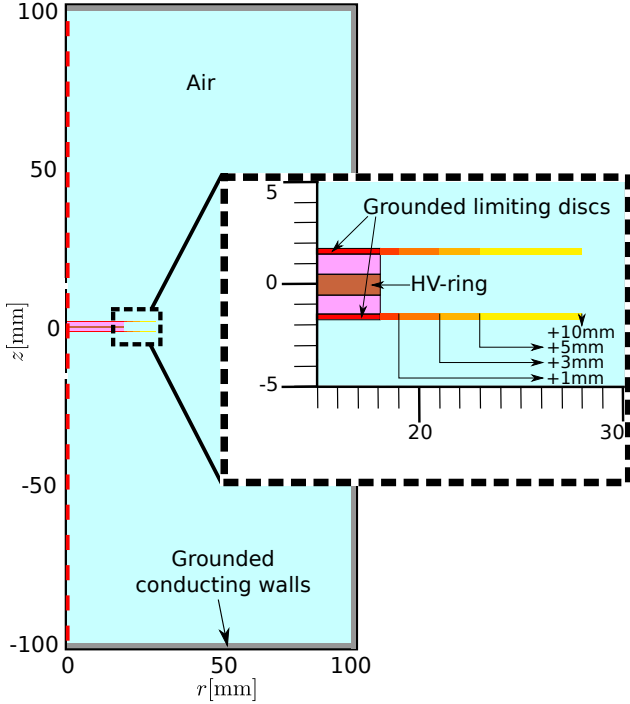


Figure 5. Schematic of the simulation geometry. The vertical dashed red line corresponds to the axis of symmetry. The vacuum chamber walls are indicated in grey. A detailed view of the SRA is depicted. The insulating components are shown in magenta. The grounded limiting discs are in red, with the increasing diameters indicated with different colours up to yellow. The HV-ring is indicated in orange.

try at $r = 0$ cm is indicated with a dashed red line. Air at different pressures is set as the medium inside a cylindrical grounded chamber of 20 cm diameter. In the middle of the chamber at $z = 0$ mm, a simplified model of the SRA is reproduced. An insulating ring is placed between the grounded limiting discs and the central HV-ring. The grounded rings of different sizes are indicated with different colours, from those with the same dimensions of the HV-ring (+0 mm, in red), up to the discs resulting in +10 mm grounded limiting surfaces, indicated in yellow.

The vacuum electric field $\vec{E} = -\vec{\nabla}V$ is calculated from the Laplace equation $\nabla^2V = 0$ and from the boundary conditions on the voltage. Space charge effects and surface charge accumulation on insulators are neglected, because of the negligible densities of electrons and ions before breakdown. In Fig. 6(a) and 6(b), the electric field intensity is illustrated for a bias of 1 kV on the HV-ring, for the configuration with +0 mm and +10 mm discs, re-

spectively. Detailed pictures of the SRA are shown in the corresponding insets. There is a significant modification of the electric field distribution when the size of the grounded limiting discs is increased. In most of the vacuum chamber volume, the E -field decreases by three orders of magnitude. Moreover, a significant fraction of the electric field lines leaving the HV-ring surface (in black) reach the wall chamber for the +0 mm setup (a). On the contrary, the field lines are confined in the space between the discs for the +10 mm configuration (b). A complementary view is given by the electric field streamlines leaving the chamber wall surface, indicated by the grey streamlines. For the +10 mm discs, these lines can reach the HV-ring surface only in a narrow central region.

The calculated field distribution is therefore consistent with the observation that breakdown is progressively suppressed on long electric field paths for increasing disc size. The grounded limiting discs are acting as partial Faraday screens for the electric field. Fluid simulations were performed to complement the experimental measurements of electrical breakdown, implementing the model presented in [2, 6, 8]. The low-pressure range was explored, increasing the diameter of the grounded limiting discs, from +0 mm up to +3 mm. The results[4] are shown in Fig. 7, showing a good qualitative agreement with the measured breakdown curves in Fig. 4 [[4]]. The curves steepen by increasing the discs diameter in the pressure range from 2×10^{-2} mbar to 1 mbar, confirming the inhibition of the electrical breakdown towards the chamber walls. Several reasons could be responsible for the quantitative differences with respect to the experimental values, such as the numerical values of Townsend's first and second ionization coefficients. Further numerical investigations will address this topic.

2.4. Biased Limiting Discs

The configuration presented in Sec. 2.2 can be optimized by varying the values of R_1 and R_2 , and therefore the potential of the limiting discs. A simplified schematic of the circuit is shown in Fig. 8. The relative bias between the central HV-ring and the limiting discs is the key parameter that determines the breakdown at high pressure on short paths. Therefore, a positive voltage on the limiting discs with respect to the reference potential of the satellite would allow to increase the value of electric potential of the central HV-ring at which the breakdown occurs. The resistances have to be chosen high enough to keep the current below the $100 \mu\text{A}$ limit of the dielectric tester that is used for breakdown detection. At the same time, the currents through R_1 and R_2 must be larger than Townsend currents, otherwise the limiting disc potential would be affected. The tested configuration features $R_1 = R_2 = 68 \text{ M}\Omega$, corresponding to a current of $\sim 7 \mu\text{A}$. The bias voltage of the limiting discs is therefore $1/2$ the value on the central ring ($V_{\text{discs}} = 0.5V_{\text{HV}}$). The measured breakdown curve with respect to the voltage applied at the central ring is shown in Fig. 9. For pressures below 0.7 mbar, we can observe breakdown voltages in the range 1 kV-2 kV, which is consistent with

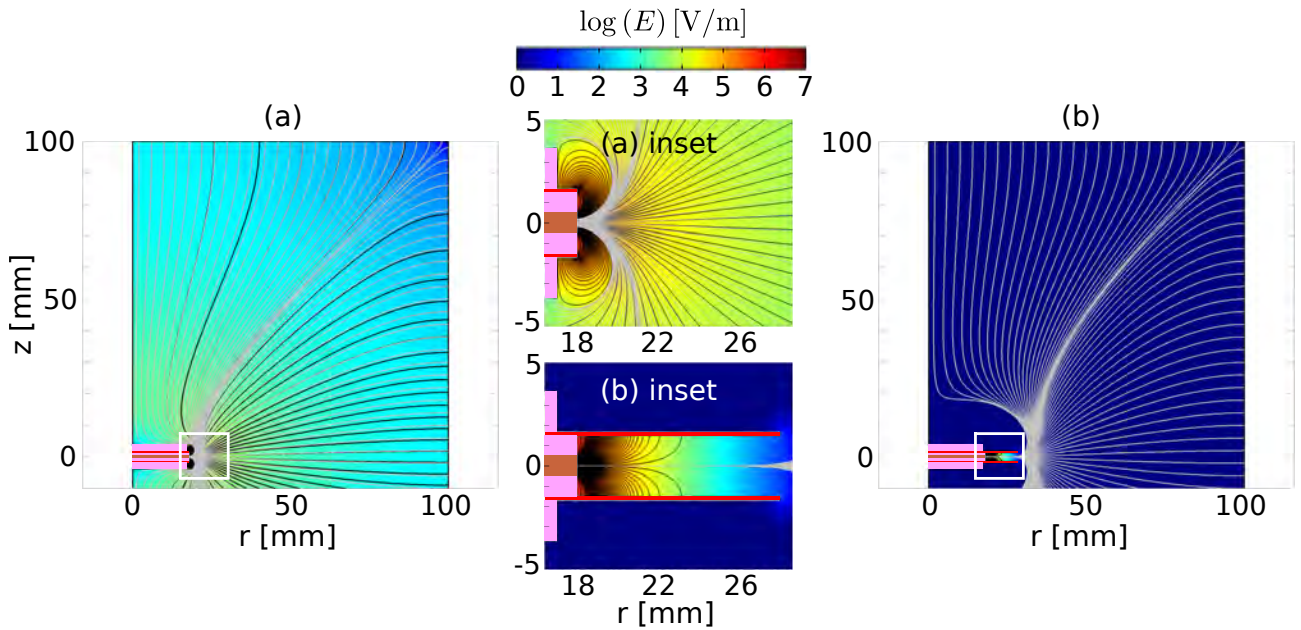


Figure 6. Electric field distribution for (a) the +0 mm, and (b) the +10 mm disc configurations. Detailed views of the corresponding slip ring assemblies are illustrated in the corresponding insets for (a) and (b) marked by the white rectangles. The electric field streamlines leaving the HV-ring surface/chamber wall surface are in black/gray, respectively.

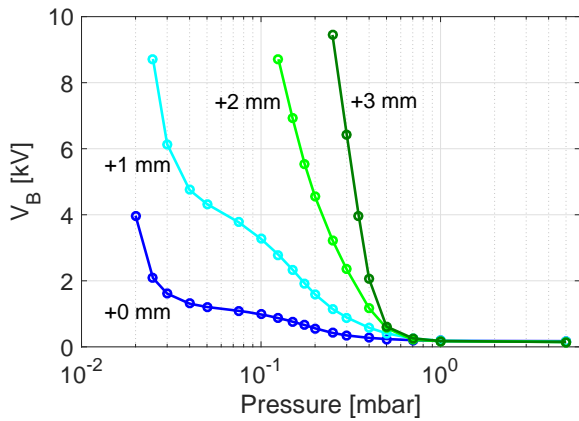


Figure 7. Numerical simulations of breakdown voltage as a function of pressure, for several diameters of the grounded limiting discs.

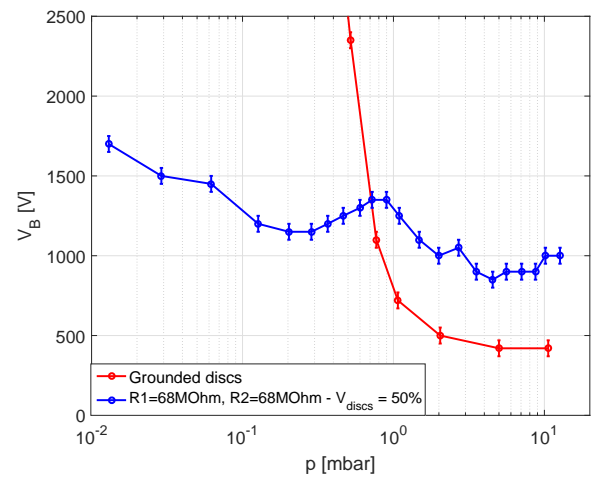


Figure 9. Comparison of breakdown curves for grounded discs (red) and for discs biased to half of the HV-ring voltage (blue).

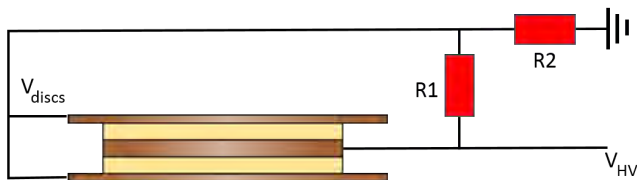


Figure 8. Schematic of a design with passively-biased limiting discs.

the possibility of having a breakdown between the biased limiting discs and the surrounding chamber. However, the measured values remain above the target volt-

age of ~ 600 V. For pressures higher than 0.7 mbar, we can observe breakdown voltages almost twice as high as the grounded solution, corresponding to the same relative potential between the central ring and the limiting discs. The minimum of the breakdown curve of the SRA mockup has therefore been increased to more than 600 V.

3. ADVANCED SRA MOCKUP

To reproduce the complex structure of a real slip ring, the advanced mockup shown in Fig. 10 has been developed. It is composed of a conducting housing and a central conducting cylindrical axis on which 36 gold-plated rings are inserted. These rings are designed to be used in groups of three, with a central HV-ring of 32 mm and two limiting discs with bigger diameter. Consecutive groups feature limiting discs of increasing size. Consecutive conducting rings are electrically separated by insulating rings of 1 mm thickness. Gold-plated brushes mounted on the insulating board on top of the housing make electrical contact with the rings. The brushes are covered with Kapton, with the exception of the tip in contact with the ring. The PCV board connects the brushes to a set of cables allowing the independent control of the potential on each ring. Measurements have been performed in a 1.5 m high,

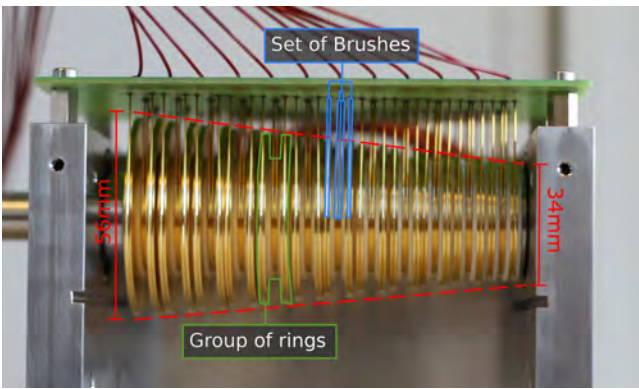


Figure 10. Picture of the advanced SRA mockup.

1.2 m wide vacuum chamber, using a LABView software that controls the pressure and the positive applied voltage via a dielectric tester, automatically acquiring the breakdown curve. A voltage ramp with a speed of 400 V/s is applied from 0 V to the maximum value of 2 kV, keeping the maximum value for 4 s. A threshold current value of $100 \mu\text{A}$ is used to detect the breakdown voltage V_B . The explored pressure value range from 10^{-1} mbar to 40 mbar, to sufficiently investigate breakdown around the minimum of the breakdown curve that is close to 1 mbar. Five values of V_B are measured for each pressure, calculating the corresponding average and standard deviation as error bar. The pressure error bar corresponds to the 15 % tolerance given to the predefined pressure values at which the breakdown is obtained.

In Fig. 11, preliminary measurements with grounded limiting discs are presented, keeping grounded the SRA housing and the others conducting rings as well. For pressure lower than 0.6 mbar, a significant increase in the breakdown voltage for the +12 mm curve is observed with respect to the +1 mm curve. This confirms the screening effect observed with the simple SRA mockup discussed in Sec.2.2. For pressures higher than 0.6 mbar, the same minimum breakdown voltage is reached, which is consistent with the presence of short-path breakdown between the HV-ring and the limiting grounded discs.

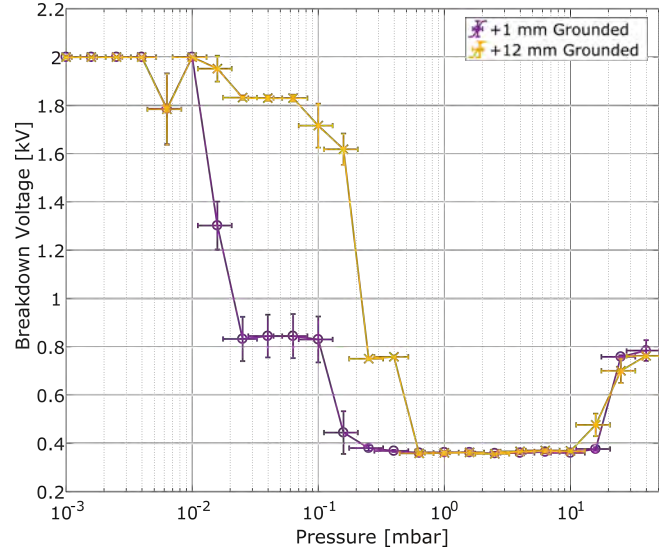


Figure 11. Breakdown curves measured on the advanced SRA mockup for two groups of grounded limiting discs, with a radius exceeding the central HV ring radius by 1 mm and 12 mm.

4. CONCLUSIONS AND OUTLOOK

In this work, innovative electric breakdown mitigation passive techniques for a satellite slip ring assembly have been presented. The key role played by the vacuum chamber, which mimics the SRA housing, has been demonstrated. The electrical breakdown between the high-voltage electrode and the surrounding conducting walls dominates the low pressure branch of the measured breakdown curve. An innovative passive technical solution has been implemented to inhibit gas breakdown at low pressures: by increasing the grounded discs diameter, the occurrence of the HV-ring breakdown against the chamber is eliminated for pressures below 1 mbar and applied voltage below 1 kV. Intuitively, the grounded discs act as a partial Faraday screen, strongly reducing the value of the electric field and limiting the range of the electric field path length to the walls. The proximity of the grounded limiting discs is counter-intuitive from the point of view of vacuum breakdown. However this approach effectively inhibits gas breakdown, occurring at much lower voltages than for vacuum breakdown. Numerical simulations based on fluid transport equations of ions and electrons confirm the effectiveness of the method. An alternative configuration with biased limiting discs is presented, to effectively increase the minimum of the whole breakdown voltage curve. This allows to reach the target of voltage operation of approximately 600 V. Finally, preliminary results with an advanced SRA are presented for the grounded limiting discs configuration, addressing the compatibility of the described approach for a real satellite slip ring. Further tests are foreseen with the biased limiting disc configuration to confirm the possibility of increasing the minimum of the breakdown voltage curve up to ~ 700 V. We note that in a real satellite

SRA, the current flowing through the limiting discs has to be kept low to minimize the power losses: for 600 V DC, a power loss of only ~ 5 mW would result for the investigated resistances of 68 M Ω .

5. ACKNOWLEDGMENTS

This work is part of the High Voltage - Electrical Power System Architecture (HV-EPISA) project and it has received funding from the SEFRI under grant agreement number 15.0340, in the framework of the European Union's Horizon 2020 research and innovation programme. The views and opinions expressed herein do not necessarily reflect those of the European Commission. The authors wish to acknowledge very helpful discussions with SPC colleague R. Jacquier, and the support of the SPC technical team.

REFERENCES

- [1] G. Bonin, N. Orr, R.E. Zee, and J. Cain, *Solar Array Arcing Mitigation for Polar Low-Earth Orbit Spacecraft*, 24th Annual AIAA/USU Conference on Small Satellites (2010).
- [2] R. Schnyder, A.A. Howling, D. Bommottet, and C. Hollenstein, *J. Phys. D: Appl. Phys.* **46**, 285205 (2013).
- [3] A. Leporini, V. Giannetti, T. Andreussi, D. Pedrini, A. Rossodivita, A. Piragino, M. Andrenucci, and D. Estublier, *Development of a 20 kW-class Hall effect thruster*, Proceedings of Space Propulsion, (2016).
- [4] F. Avino, P. Martens, A. Howling, D. Bommottet, and I. Furno, *Gas breakdown investigation and mitigation in satellite slip rings*, submitted to Aerospace Science and Technology.
- [5] RUAG Space Switzerland Nyon (RSSN), slip ring.
- [6] R. Schnyder, *DC Breakdown in gases for complex geometries from high vacuum to atmospheric pressure*, EPFL Lausanne, Switzerland, PhD thesis n $^{\circ}$ 5962 (2013).
- [7] COMSOL Inc. and www.comsol.com.
- [8] N. Leoni, and B. Paradkar, Proc. IS&T's NIP (Springfield, VA), p229 (2009).